

201313057A

別添1

厚生労働科学研究費補助金  
第3次対がん総合戦略研究事業

国際協調に基づく日本人難治がんゲノムデータベースの構築  
(国際がんゲノムコンソーシアム研究)

平成25年度 総括・分担研究報告書

研究代表者 柴田 龍弘

平成26(2014)年 5月

## 目次

I. 総括研究報告	
国際協調に基づく日本人難治がんゲノムデータベースの構築	----- 1
柴田 龍弘	
II. 分担研究報告	
国際協調に基づく日本人難治がんゲノムデータベースの構築	----- 4
油谷 浩幸	
III. 研究成果の刊行に関する一覧表	----- 7
IV. 研究成果の刊行物・別刷	

厚生労働科学研究費補助金（第3次対がん総合戦略研究事業）

総括研究報告書

国際協調に基づく日本人難治がんゲノムデータベースの構築

（国際がんゲノムコンソーシアム研究）

研究代表者 柴田 龍弘 国立がんセンター研究所

がんゲノミクス研究分野・分野長

研究要旨

本研究グループが主体となった国際共同研究により 600 例を超える肝がんゲノム解読データを集積・解析することで、世界最大の肝がんゲノム解析研究を達成し、新たな治療標的を含めた包括的な肝がんゲノム解読研究を進めた。とりわけ TERT 遺伝子の活性化が 70%以上の症例で観察されたことから、TERT 遺伝子の異常を標的とした早期診断や治療開発が肝がんにおいて極めて重要であることが明らかとなった。希少かつ難治がんである胆道がんにおいて治療標的として有望な FGFR2 融合遺伝子、びまん性胃癌において高頻度に変異が生じている分子を新たに発見した。国際がんゲノムコンソーシアムにおける共同研究として、30 種類のがん、7000 症例における体細胞変異ビッグデータを解析することで、20 種類を超える特徴的な変異パターンの存在を発見し、発がん要因との関連について同定した。

A. 研究目的

最新のゲノムシーケンス解析技術を駆使し、日本人に特徴的かつ健康対策上重要な固形がん（肝がん・胆道がん・低分化胃がん）におけるがんゲノム・エピゲノム異常を包括的・統合的に解析し、疫学的因子との関連や新たな治療標的の同定を進める。国際がんゲノム解析共同体に参加し、その標準化手順に従ってがんゲノム解析データを公開し、国際貢献を目指す。微小検体解析技術等の新技術開発を進め、新たな分子診断・治療法開発・実用化を目指す。

B. 研究方法

1. がん全エクソンシーケンス

413 例の肝がん症例並びに同一患者の非腫瘍肝臓から DNA を抽出し、SureSelectXT Human All Exon V4 Kit を用いて、エクソン領域を濃縮後、Illumina HiSeq2000 によって、少なくとも x100 以上のカバー率でシーケンス解読を行った。独自に構築したアルゴリズムを用いて、体細胞変異の同定、コピー数変化・腫瘍含有率を算出し、腫瘍量に応じた補正を加え、腫瘍内における変異アレル頻度の算出を行った。体細胞変異データは、国際がんゲノムコンソーシアムのデータベースに登録し、その情報を公開した。

2. がんトランスクリプトーム解読

KRAS/BRAF 変異を有しない胆道がん臨床検体（8 例）から RNA を抽出し cDNA を合成後、同様に Illumina HiSeq2000 を用いて全転写産物のシーケ

ンス解読を行った。肺がん融合遺伝子同定で実績のあるアルゴリズムを用いて、融合遺伝子の検出、mRNA 並びに非コード RNA の発現変化、異常スプライシングなどを網羅的に検出した。

更に発見した FGFR2 融合遺伝子を NIH3T3 細胞に導入し、軟寒天内コロニー形成や免疫不全マウスへの移植実験によってがん遺伝子としての活性を測定した。樹立した細胞株を用いて、低分子 FGFR2 阻害剤添加による in vitro における増殖抑制を測定した。

3. がんゲノム情報解析

6 種類の体細胞塩基置換 (T>G/A>C, T>C/A>G, T>A/A>T, C>T/G>A, C>A/G>T, C>G/G>C) を、更にその前後の塩基 (T, C, G, A) の情報を加味することで、96 (=4x6x4) 種類のマトリックスに分類し、主成分解析、非負値行列因子分解等によって解析し、変異パターンの抽出や、臨床情報との相関について検討を行った。変異・コピー数異常データを統合し、分子経路ごとの濃縮といった pathway 解析を行い、重要な分子経路の同定を進めた。

（倫理面への配慮）

本研究は疫学研究の指針に基づき国立がんセンター倫理審査委員会にて承認を得た上で研究を進めた。臨床検体の提供者には、臨床検体が医学研究に使われることについて文書および口頭で説明し、臨床検体は連結可能匿名化を行い、個人を特定することができるような情報はいっさい付加されずに実験に使

用した。国立がんセンターの実験動物倫理委員会の指針およびカルタヘナ法のもと、動物の愛護および管理に関する法律、実験動物の飼養および保管等に関する基準にしたがって行った。

## C. 研究結果

### 1) 600 例を超える肝がんのゲノム解析

日本人肝がん症例 413 例並びに米国人肝がん症例 90 例 (米国ペイラー医科大学との共同研究) の合計 503 例について全エクソーム解読を行い、体細胞突然変異、コピー数異常、B 型肝炎ウイルスゲノム挿入部位を包括的に同定した。その結果、TERT 遺伝子異常 (プロモーター変異、遺伝子増幅、TERT 遺伝子座への B 型肝炎ウイルスゲノム挿入) を 70% 以上の症例で認めた。既知の TP53, WNT 経路、クロマチンリモデリング分子群に加えて、mTOR 阻害剤の標的として有望な TSC1/2、HGF 経路の活性化を制御するプロテアーゼである TMPRSS13、更に全く新しい機能グループとして代謝経路制御分子群 (G6PC, ADH1B 等) の異常を発見した。

更に米国がんゲノムプロジェクト (TCGA) と共同研究を進め、米国肝がん 105 例のデータを追加し、合計 608 例の肝がんゲノムデータを集積・解析することで、特徴的な体細胞塩基置換パターンが、ウイルスの種類ではなく、人種の違い (日本人、白人、米国在住アジア系) と強く相関することを世界で初めて発見した。

### 2) 胆道がんにおける新規キナーゼ融合遺伝子の発見と臨床開発の促進

希少がんでありかつ難治がんであるため、これまで有効な治療法の開発が進んでいなかった胆道がんについて、RNA シークエンスを行ない、網羅的な融合遺伝子探索を行った。その結果、治療標的として有望な FGFR2-AHCYL1, FGFR2-BICC1 という新たなキナーゼ融合遺伝子を肝内胆管がんの約 15% の症例で同定した。これらの融合遺伝子は *in vitro* 並びに *in vivo* において、がん遺伝子としての活性を示し、更に低分子 FGFR 阻害剤によって増殖抑制を認めた。現在複数の製薬会社が FGFR 阻害剤の臨床試験を進めており、胆道がんにおける臨床開発を促進するために、国立がん研究センター中央病院肝胆腫内科と共に全国レベルの多施設スクリーニング体制 (BT-SCRUM) の構築を進めた。

### 3) 低分化胃がんにおける新規ゲノム異常の同定

低分化胃がんのゲノム解析に関する予備的検討として 30 例のエクソーム解析を実施し、更に追加の低分化胃がん 57 症例についてターゲットシーケンス解析を実施したところ、高頻度 (22/87) で変異を来す新規治療標的分子を同定した。本遺伝子変異は高分化型の腸型胃癌 51 症例には検出されず、びまん性胃癌に特徴的な変異であると思われた。変異を有する細胞株に対して当該分子 siRNA によるノックダウンを行なった結果、コントロール群と比較して約 75% の細胞増殖抑制効果が認められた。

### 4) 横断的がんゲノム変異パターンの解析

国際がんゲノムコンソーシアムにおける共同研究として、30 種類のがん、7000 症例における体細胞変異ビッグデータを解析することで、20 種類を超える特徴的な変異パターンの存在を発見した。これらの約半数は、加齢、喫煙、DNA ミスマッチ異常、BRCA1 異常といった発がん要因と相関することが明らかとなり、がんゲノム解析と発がん因子との密接な関連を解明した。残りの置換パターンは原因が未知であるため、こうした解析から新たな発がん要因の同定と予防研究への展開が期待される。

## D. 考察

### 1) 包括的な肝がんゲノム異常解析

本研究グループが主体となった国際共同研究により 600 例を超える肝がんゲノム解読データを集積・解析することで、現時点で最大の肝がんゲノム解析研究を達成し、新たな治療標的を含めた包括的な肝がんゲノム解読研究を進めた。とりわけ TERT 遺伝子の活性化が 70% 以上の症例で観察されたことから、TERT 遺伝子の異常を標的とした早期診断や治療開発が肝がんにおいて極めて重要であることが明らかとなった。

### 2) 胆道がんにおける新規治療標的の同定

希少かつ難治がんである胆道がんにおいて FGFR2 融合遺伝子を新たに発見した。FGFR2 融合遺伝子はがん遺伝子としての活性を呈し、かつ低分子 FGFR2 阻害剤による増殖抑制を示すことから、治療標的として有望と考えられる。現在 FGFR2 融合遺伝子を対象とした分子診断並びに臨床試験を目指した臨床研究を開始している。

### 3) 低分化胃がんにおける新規ゲノム異常の同定

予後不良とされるびまん性胃癌において高頻度に変異が生じている分子が同定されたことにより、関与する増殖シグナルを標的とする治療薬の開発が期待されると共に、変異の有無と既存治療法の奏功性との関連についても研究の展開が期待される。

### 4) がん種横断的な塩基置換解析と発がん研究への展開

がんゲノムビッグデータを解析することで、体細胞塩基置換における主要なパターンの同定と発がん要因との関連について研究を進める事ができた。今後こうしたデータと、様々な臨床背景との解析によって、新たな発がん要因の同定や効果的ながん予防研究を推進するための重要な情報基盤が出来上がっていくと期待される。

## E. 結論

600 例を超える肝がんゲノム解読データから TERT 遺伝子を含み、診断・治療法の開発において有望な遺伝子を網羅的に同定することができた。更に分子経路解析等新たな手法によって、肝がんにお



ける分子ネットワークの解明に一步近づく事ができた。今後、ゲノム変異・発現データに加え、エピゲノム異常データを追加することで、より統合的な分子解析を進める。TERT 遺伝子の異常を標的とした早期診断や治療開発が肝がんにおいて極めて重要であり、臨床開発に乗り出す。

難治がんである胆道がんにおける FGFR2 融合遺伝子並びに低分化胃がんにおける高頻度新規ゲノム異常の発見は、今後の該当疾患の治療体系を大きく変える可能性がある。これらの疾患は、日本を始め東アジアで頻度の高いがんであることから、今回の発見を起点として臨床開発においてもアジアにおいて主導的な役割を担うように継続的な研究が望まれる。すでに FGFR2 融合遺伝子を対象とした分子診断並びに臨床試験を目指した臨床研究を開始している。

F. 健康危険情報  
特になし

G. 研究発表

1. 論文発表

- 1) Alexandrov LB, Nik-Zainal S, Wedge DC, Aparicio S, Behjati S, Biankin AV, Bignell GR, Bolli N, Borg A, Borresen-Dale A, Boyault S, Burkhardt B, Butler AP, Caldas C, Davies HR, Desmedt C, Elis R, Eyfjoro JE, Foekens JA, Greaves M, Hosoda F, Huter B, Illicic T, Imbeaud S, Imielinski M, Jager N, Jones DTW, Jones D, Knappskog S, Kool M, Lakhani SR, Lopez-Otin C, Martin S, Munshi NC, Nakamura H, Northcott PA, Pajic M, Papaemmanuil E, Paradiso A, Pearson JV, Puente XS, Raine K, Ramakrishna M, Richardson AL, Richter J, Rosenstiel P, Schlessner M, Span PN, Teague JW, Totoki Y, Tutt A, Valdes-Mas R, van't Veer L, Vincent-Salomon A, Waddell N, Yates LR, Zucman-Rossi J, Futreal AP, McDermott U, Lichter P, Meyerson M, Grimmond S, Siebert R, Campo E, **Shibata T**, Pfister SM, Campbell P, Stratton MR. Signatures of mutational processes in human cancer. *Nature* 500:415-421, 2013
- 2) **Shibata T**, Aburatani H. Exploration of liver cancer genomes. *Nat Rev Gastroenterol Hepatol.*, 2014 doi: 10.1038/nrgastro.2014.6. [Epub ahead of print]
- 3) Arai Y, Totoki Y, Hosoda F, Shirota T, Hama N, Nakamura H, Ojima H, Furuta K, Shimada K, Okusaka T, Kosuge T, **Shibata T**. FGFR2 tyrosine kinase fusions define a unique molecular subtype of cholangiocarcinoma. *Hepatology* 59:1427-1434, 2014.

2. 学会発表

1. がん研究分野の特性等を踏まえた支援活動公開シンポジウム講演 (平成 25 年 8 月 22 日)  
「シーケンス解読によって明らかになった新たながんゲノム像」
2. 第 24 回 日本消化器癌発生学会総会 (平成 25 年 9 月 6 日) 講演 「胆道がんにおける新規

融合遺伝子の同定」

3. 日本癌学会 International Session 3 講演  
「Evaluation of cancer genome sequencing towards personalized molecular diagnosis」(平成 25 年 10 月 5 日)
  4. がん新薬開発合同シンポジウム講演 (平成 25 年 11 月 29 日)「国際がんゲノムコンソーシアムでのゲノム解析の成果と今後の方向性」
  - 4.
- H. 知的財産権の出願・登録情報

FGFR2 融合遺伝子 (特願 2012-151352)

厚生労働科学研究費補助金(第3次対がん総合戦略研究事業)  
分担研究報告書

国際協調に基づく日本人難治がんゲノムデータベースの構築(国際がんゲノムコンソーシアム研究)  
に関する研究

研究分担者 油谷浩幸 東京大学先端科学技術研究センター 教授

**研究要旨**

肝がん・低分化胃がんにおけるがんゲノム・エピゲノム異常を包括的・統合的に解析し、新たな治療標的の同定を進めた。国際がんゲノムコンソーシアムにおける大規模解析に参加し、国際連携に貢献した。

**A. 研究目的**

最新のゲノムシーケンス解析技術を駆使し、日本人に特徴的かつ健康対策上重要な固形がん(肝がん・低分化胃がん)におけるがんゲノム・エピゲノム異常を包括的・統合的に解析し、疫学的因子との関連や新たな治療標的の同定を進める。国際がんゲノム解析共同体における大規模解析に参加し、国際連携・貢献を果たす。

**B. 研究方法**

**1. 肝細胞がんのゲノム解析**

エクソーム解析データについてがん研究センターおよび米国ベイラー大学ゲノム研究センターのグループと共同で解析を実施した。エクソーム解析で同定された頻度の高い体細胞変異についてはAmpliSeqにより増幅した産物をIon PI chip v2によりIon Proton(Life Technology)で配列決定した。

さらにRNA-seqにより、進行がん156検体、非癌部64検体に対して鎖特異的に100塩基ペアエンドのトランスクリプトームデータが得られた。エクソーム解析を実施した症例についてRNA-seq解析およびDNAメチル化解析を実施した。メチル化解析に関しては当センターが収集した266例(うち癌部210、非癌部56)、理化学研究所267

例、がん研究センター236例の769検体について、HumanMethylation450 BeadChip(イルミナ社)を用いて解析した。

**2. 低分化型胃がんのゲノム解析**

難治性である低分化型胃がんにおける新規治療標的を同定するために、東京大学医学部附属病院で収集された30症例の癌部および非癌部からマクロダイセクションにより抽出したゲノムDNAについて、SureSelect(Agilent)試薬を用いて濃縮した全エクソン領域の配列解析を100塩基ペアエンドでHiSeq2000(イルミナ)を用いて実施した。

さらに低分化胃がん57例、腸型胃がん51例についてTruSeqカスタムアンプリコン試薬(イルミナ)を用いて46遺伝子のターゲットシーケンスをMiSeq(イルミナ)により200塩基ペアエンドで実施した。

(倫理面への配慮)

本研究計画については組織検体採取および検体解析に関して東京大学医学部附属病院および日本大学附属板橋病院における倫理委員会において承認を受けた。

## C. 研究結果

### 1. 肝細胞がんの統合ゲノム解析

エクソーム解析で同定された変異の97.4 % (1021/1048)がIonProtonを用いた解析で確認された。

トランスクリプトームデータからキメラRNAの検出を行い、同じ遺伝子の組み合わせで繰り返し転座が認められた候補についてRT-PCR法による確認を進めた。

Infiniumアレイを用いて45万箇所のCpGサイトのメチル化レベルに関して、713症例のプロファイルが得られた。

### 2. 低分化型胃がんのゲノム解析

低分化胃がんのゲノム解析に関する予備的検討として30例のエクソーム解析を実施し、本研究室で開発した解析パイプラインであるKarkinosを用いて塩基変異、コピー数変異解析を行ったところ、癌部102x、正常部99xのリード深度が得られ、6,616の体細胞変異(一塩基変異5,359, indel 1,257)が同定された。

追加の低分化胃がん57症例についてターゲットシーケンス解析を実施したところ、高頻度(22/87)で変異を来す新規治療標的分子を同定した。本遺伝子変異は高分化型の腸型胃癌51症例には検出されず、びまん性胃癌に特徴的な変異であると思われた。変異を有する細胞株に対して当該分子 siRNA によるノックダウンを行なった結果、コントロール群と比較して約75%の細胞増殖抑制効果が認められた。

## D. 考察

肝細胞がんについて同一検体から体細胞変異、トランスクリプトーム、メチル化のデータが得られたことにより、今後統合ゲノム解析を行う予定である。

予後不良とされるびまん性胃癌において高頻度に変異が生じている分子が同定されたことにより、関与する増殖シグナルを標的とする治療薬の開発が期待されると共に、変異の有無と既存治療法の奏功性との関連についても研究の展開が期待される。

## E. 結論

肝細胞がんの統合ゲノム解析のためのデータが得られた。難治性とされる低分化型胃癌において高頻度な変異遺伝子を同定した。

## F. 健康危険情報

## G. 研究発表

### 1. 論文発表

- 1) Hayashi A, Yamauchi N, Shibahara J, Kimura H, Morikawa T, Ishikawa S, Nagae G, Nishi A, Sakamoto Y, Kokudo N, Aburatani H, Fukayama M. Concurrent Activation of Acetylation and Tri-Methylation of H3K27 in a Subset of Hepatocellular Carcinoma with Aggressive Behavior. PLoS One. 9(3):e91330. 2014
- 2) 油谷浩幸 “ゲノム変異解析” 雑感 医学のあゆみ 245(5): 471-475, 2013
- 3) 油谷浩幸 次世代高速シーケンサー技術の成果からみた消化器癌個別化医療の将来は 分子消化器病 10(4):354-361, 2013
- 4) 油谷浩幸 がんゲノムプロジェクト 実験医学 31(15):2438-2445, 2013
- 5) 油谷浩幸 エピゲノム解析法 遺伝子医学 MOOK 25: 50-54, 2013
- 6) 油谷浩幸 「網羅的解析研究」雑記帳 血管医学 14(4):411-417, 2013

### 2. 学会発表

- 1) 油谷浩幸 第17回日本がん分子標的治療学会学術集会(6/13/2013) Year in review 「がんゲノム解析と分子標的治療」
- 2) 油谷浩幸 第11回日本臨床腫瘍学会学術集会(8/31/2013)教育講演:Latest Medical Care「Tumor profiling in clinical practice」
- 3) 油谷浩幸 第13回東北がん分子標的治療研究会(11/15/2013)「がんゲノム解析の現状と医療応用へ向けての課題」

## H. 知的財産権の出願・登録状況(予定も含む)

1.特許取得

なし

2.実用新案登録

なし

3.その他

## 研究成果の刊行に関する一覧表

## 書籍

著者氏名	論文タイトル名	書籍全体の 編集者名	書 籍 名	出版社名	出版地	出版年	ページ
	該当なし						

## 雑誌

発表者氏名	論文タイトル名	発表誌名	巻号	ページ	出 版 年
Alexandrov LB, Shibata T, et al.	Signatures of mutational processes in human cancer.	Nature	500 (7463)	415-421	2013
Shibata T, Aburatani H	Exploration of liver cancer genomes.	Nat Rev Gastroenter ol Hepatol		In press	2014
Arai Y, Tototki Y, Hosoda F, Shirota T, Hama N, Nakamura H, Ojima H, Furuta K, Shimada K, Okusaka T, Kosuge T, Shibata T.	FGFR2 tyrosine kinase fusions define a unique molecular subtype of cholangiocarcinoma.	Hepatology	59(4)	1427-143 4	2014
Hayashi A, Yamauchi N, Shibahara J, Kimura H, Morikawa T, Ishikawa S, Nagae G, Nishi A, Sakamoto Y, Kokudo N, Aburatani H, Fukayama M.	Concurrent Activation of Acetylation and Tri-Methylation of H3K27 in a Subset of Hepatocellular Carcinoma with Aggressive Behavior.	PLoS One	9(3)	e91330	2014

# Signatures of mutational processes in human cancer

A list of authors and their affiliations appears at the end of the paper

All cancers are caused by somatic mutations; however, understanding of the biological processes generating these mutations is limited. The catalogue of somatic mutations from a cancer genome bears the signatures of the mutational processes that have been operative. Here we analysed 4,938,362 mutations from 7,042 cancers and extracted more than 20 distinct mutational signatures. Some are present in many cancer types, notably a signature attributed to the APOBEC family of cytidine deaminases, whereas others are confined to a single cancer class. Certain signatures are associated with age of the patient at cancer diagnosis, known mutagenic exposures or defects in DNA maintenance, but many are of cryptic origin. In addition to these genome-wide mutational signatures, hypermutation localized to small genomic regions, 'kataegis', is found in many cancer types. The results reveal the diversity of mutational processes underlying the development of cancer, with potential implications for understanding of cancer aetiology, prevention and therapy.

Somatic mutations found in cancer genomes<sup>1</sup> may be the consequence of the intrinsic slight infidelity of the DNA replication machinery, exogenous or endogenous mutagen exposures, enzymatic modification of DNA, or defective DNA repair. In some cancer types, a substantial proportion of somatic mutations are known to be generated by exposures, for example, tobacco smoking in lung cancers and ultraviolet light in skin cancers<sup>2</sup>, or by abnormalities of DNA maintenance, for example, defective DNA mismatch repair in some colorectal cancers<sup>3</sup>. However, our understanding of the mutational processes that cause somatic mutations in most cancer classes is remarkably limited.

Different mutational processes often generate different combinations of mutation types, termed 'signatures'. Until recently, mutational signatures in human cancer have been explored through a small number

of frequently mutated cancer genes, notably *TP53* (ref. 4). Although informative, these studies have limitations. To generate a mutational signature, a single mutation from each cancer sample is entered into a mutation set aggregated from several cases of a particular cancer type. A signature that contributes the large majority of somatic mutations in the tumour class is accurately reported. However, if multiple mutational processes are operative, a jumbled composite signature is generated. Furthermore, because such studies are based on 'driver' mutations<sup>1</sup>, signatures of selection are superimposed on the signatures of mutational processes.

Recent advances in sequencing technology have overcome past limitations of scale<sup>1</sup>. Thousands of somatic mutations can now be identified in a single cancer sample, offering the possibility of deciphering mutational signatures even when several mutational processes are

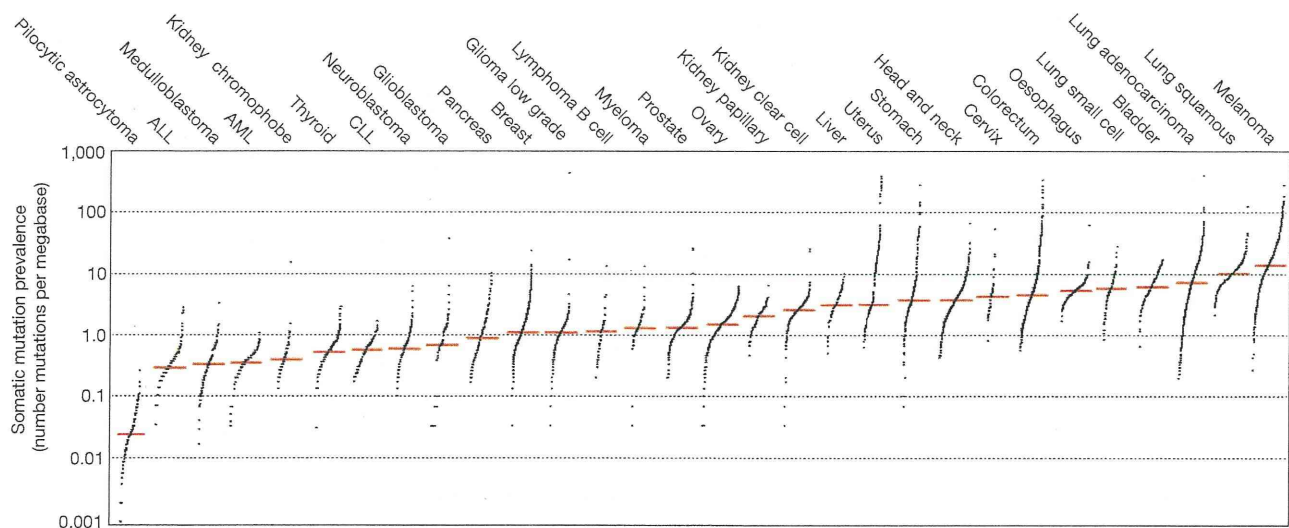


**Figure 1** | The prevalence of somatic mutations across human cancer types. Every dot represents a sample whereas the red horizontal lines are the median numbers of mutations in the respective cancer types. The vertical axis (log scaled) shows the number of mutations per megabase whereas the different

cancer types are ordered on the horizontal axis based on their median numbers of somatic mutations. We thank G. Getz and colleagues for the design of this figure<sup>26</sup>. ALL, acute lymphoblastic leukaemia; AML, acute myeloid leukaemia; CLL, chronic lymphocytic leukaemia.





**Figure 2 | Validated mutational signatures found in human cancer.** Each signature is displayed according to the 96 substitution classification defined by the substitution class and sequence context immediately 3' and 5' to the mutated base. The probability bars for the six types of substitutions are displayed in different colours. The mutation types are on the horizontal axes,

whereas vertical axes depict the percentage of mutations attributed to a specific mutation type. All mutational signatures are displayed on the basis of the trinucleotide frequency of the human genome. A higher resolution of each panel is found respectively in Supplementary Figs 2–23. Asterisk indicates mutation type exceeding 20%.

operative. Moreover, because most mutations in cancer genomes are 'passengers'<sup>1</sup> they do not bear strong imprints of selection.

We recently developed an algorithm to extract mutational signatures from catalogues of somatic mutations and applied it to 21 breast cancer whole-genome sequences<sup>5,6</sup>. Novel and known signatures were revealed, with the contribution of each signature to each cancer sample and the timing of its activity estimated<sup>6,7</sup>. Further studies have demonstrated that the approach can also be applied, albeit with less power, to mutational catalogues from sequences of all coding exons (exomes)<sup>5</sup>. Global sequencing initiatives are now yielding catalogues of somatic mutations from thousands of cancers<sup>8</sup>. We have therefore applied this method to survey the repertoire of mutational signatures and processes operating across the spectrum of human neoplasia.

### Mutational catalogues

We compiled 4,938,362 somatic substitutions and small insertions/deletions (indels) from the mutational catalogues of 7,042 primary cancers of 30 different classes (507 from whole genome and 6,535 from exome sequences) (Supplementary Fig. 1). In all cases, normal DNA

from the same individuals had been sequenced to establish the somatic origin of variants.

The prevalence of somatic mutations was highly variable between and within cancer classes, ranging from about 0.001 per megabase (Mb) to more than 400 per Mb (Fig. 1). Certain childhood cancers carried fewest mutations whereas cancers related to chronic mutagenic exposures such as lung (tobacco smoking) and malignant melanoma (exposure to ultraviolet light) exhibited the highest prevalence. This variation in mutation prevalence is attributable to differences between cancers in the duration of the cellular lineage between the fertilized egg and the sequenced cancer cell and/or to differences in somatic mutation rates during the whole or parts of that cellular lineage<sup>1</sup>.

### The landscape of mutational signatures

In principle, all classes of mutation (such as substitutions, indels, rearrangements) and any accessory mutation characteristic, for example, the sequence context of the mutation or the transcriptional strand on which it occurs, can be incorporated into the set of features by which a mutational signature is defined. In the first instance, we extracted mutational

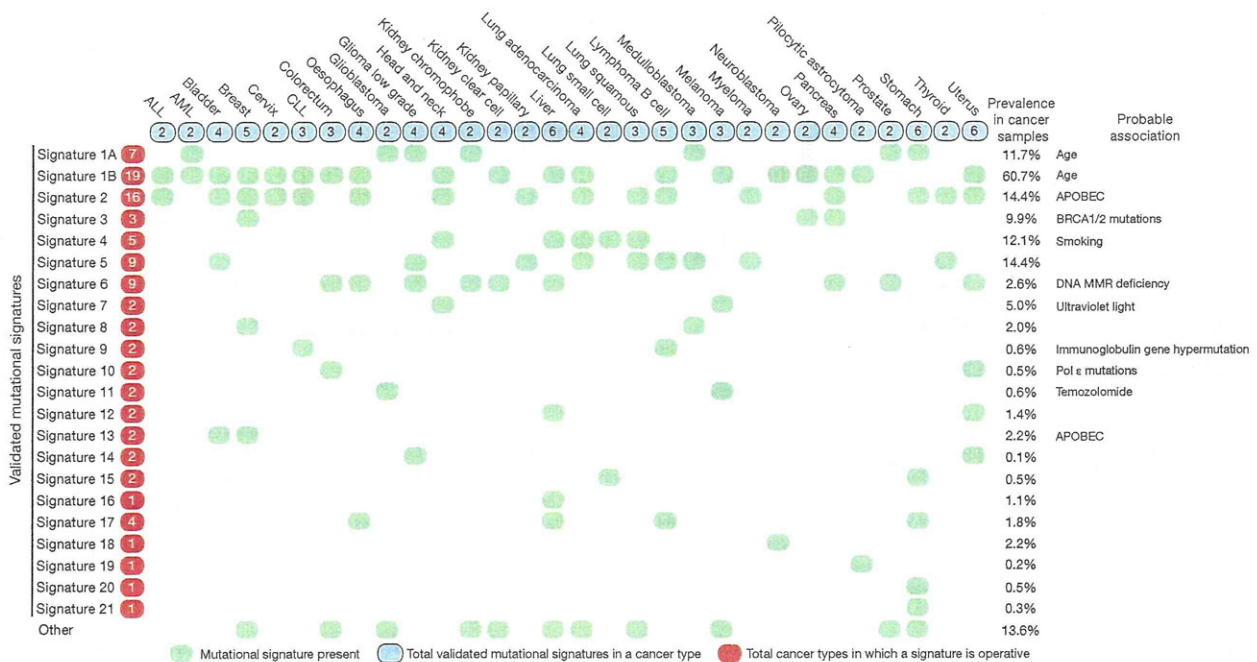


**Figure 3 | The presence of mutational signatures across human cancer types.** Cancer types are ordered alphabetically as columns whereas mutational signatures are displayed as rows. ‘Other’ indicates mutational signatures for which we were not able to perform validation or for which validation failed (Supplementary Figs 24–28). Prevalence in cancer samples indicates the

percentage of samples from our data set of 7,042 cancers in which the signature contributed significant number of somatic mutations. For most signatures, significant number of mutations in a sample is defined as more than 100 substitutions or more than 25% of all mutations in that sample. MMR, mismatch repair.

signatures using base substitutions and additionally included information on the sequence context of each mutation. Because there are six classes of base substitution—C>A, C>G, C>T, T>A, T>C, T>G (all substitutions are referred to by the pyrimidine of the mutated Watson–Crick base pair)—and as we incorporated information on the bases immediately 5′ and 3′ to each mutated base, there are 96 possible mutations in this classification. This 96 substitution classification is particularly useful for distinguishing mutational signatures that cause the same substitutions but in different sequence contexts.

Applying this approach to the 30 cancer types revealed 21 distinct validated mutational signatures (Supplementary Table 1 and Supplementary Figs 2–28). These show substantial diversity (Fig. 2 and Supplementary Figs 2–23). There are signatures characterized by prominence of only one or two of the 96 possible substitution mutations, indicating remarkable specificity of mutation type and sequence context (signature 10). By contrast, others exhibit a more-or-less equal representation of all 96 mutations (signature 3). There are signatures characterized predominantly by C>T (signatures 1A/B, 6, 7, 11, 15, 19), C>A (4, 8, 18), T>C (5, 12, 16, 21) and T>G mutations (9, 17), with others showing distinctive combinations of mutation classes (2, 13, 14).

Signatures 1A and 1B were observed in 25 out of 30 cancer classes (Fig. 3). Both are characterized by prominence of C>T substitutions at NpCpG trinucleotides. Because they are almost mutually exclusive among tumour types they probably represent the same underlying process, with signature 1B representing less efficient separation from other signatures in some cancer types. Signature 1A/B is probably related to the relatively elevated rate of spontaneous deamination of 5-methyl-cytosine which results in C>T transitions and which predominantly occurs at NpCpG trinucleotides<sup>9</sup>. This mutational process operates in the germ line, where it has resulted in substantial depletion of NpCpG sequences, and in normal somatic cells<sup>10</sup>.

Signature 2 is characterized primarily by C>T and C>G mutations at TpCpN trinucleotides and was found in 16 out of 30 cancer types

(Fig. 3). On the basis of similarities in mutation type and sequence context we previously proposed that signature 2 is due to over activity of members of the APOBEC family of cytidine deaminases, which convert cytidine to uracil, coupled to activity of the base excision repair and DNA replication machineries<sup>6,11</sup>.

In most cancer classes at least two mutational signatures were observed, with a maximum of six in cancers of the liver, uterus and stomach. Although these differences may, in part, be attributable to differences in the power to extract signatures, it seems likely that some cancers have a more complex repertoire of mutational processes than others.

Most individual cancer genomes exhibit more than one mutational signature and many different combinations of signatures were observed (Fig. 4 and Supplementary Figs 29–88). The patterns of contribution to individual cancer samples vary markedly between signatures. Signature 1A/B contributes relatively similar numbers of mutations to most cancer cases whereas other signatures contribute overwhelming numbers of mutations to some cancer samples but very few to others of the same cancer class, for example, signatures 2, 3, 4, 6, 7, 9, 10, 11, 13 (Fig. 4).

### Mutational signatures and age of cancer diagnosis

We examined each cancer type for correlations between age of diagnosis and the number of mutations attributable to each signature in each sample. Signature 1A/B exhibited strong positive correlations with age in the majority of cancer types of childhood and adulthood (Supplementary Table 2). No other mutational signature showed a consistent correlation with age of diagnosis.

The mutations in a cancer genome may be acquired at any stage in the cellular lineage from the fertilized egg to the sequenced cancer cell. The correlation with age of diagnosis is consistent with the hypothesis that a substantial proportion of signature 1A/B mutations in cancer genomes have been acquired over the lifetime of the cancer patient, at a relatively constant rate that is similar in different people, probably in normal somatic tissues. The absence of consistent correlation of all



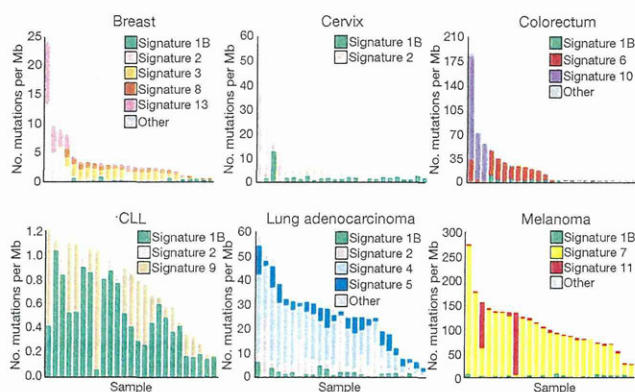


**Figure 4 | The contributions of mutational signatures to individual cancers of selected cancer types.** Each bar represents a typical selected sample from the respective cancer type and the vertical axis denotes the number of mutations per megabase. Contributions across all cancer samples could be found in Supplementary Figs 29–58. Summary of the total contributions for all operative mutational processes in a cancer type can be found in Supplementary Figs 59–88. ‘Other’ indicates mutational signatures for which we were not able to perform validation or for which validation failed (Supplementary Figs 24–28).

other signatures with age suggests that mutations associated with these have been generated at different rates in different people, possibly as a consequence of differing carcinogen exposures or after neoplastic change has been initiated.

### Mutational signatures with transcriptional strand bias

The efficiency of DNA damage and DNA maintenance processes can differ between the transcribed and untranscribed strands of genes. The most well known cause of this phenomenon is transcription-coupled nucleotide excision repair (NER) that operates predominantly on the transcribed strand of genes and is recruited by RNA polymerase II when it encounters bulky DNA helix-distorting lesions<sup>12</sup>.

We re-extracted substitution mutational signatures incorporating the transcriptional strand on which each mutation has taken place. Because a mutation in a transcribed genomic region may be either on the transcribed or the untranscribed strand, this generates a classification with 192 mutation subclasses.

Several signatures showed substantial differences in mutation prevalence between transcribed and untranscribed strands (known as transcriptional strand bias) (Fig. 5 and Supplementary Figs 89–95). For example, signature 4 shows transcriptional strand bias for C>A mutations (Fig. 5). Signature 4 is observed in lung adeno, squamous and small cell carcinomas, head and neck squamous, and liver cancers (Fig. 3), most of which are known to be caused by tobacco smoking. Therefore, signature 4 is probably an imprint of the bulky DNA adducts generated by polycyclic hydrocarbons found in tobacco smoke and their removal by transcription-coupled NER<sup>13</sup>. The higher prevalence of C>A mutations on transcribed compared to untranscribed strands is consistent with the propensity of many tobacco carcinogens to form adducts on guanine.

Similarly, signature 7, mainly found in malignant melanoma, shows a higher prevalence of C>T mutations on the untranscribed compared to the transcribed strands consistent with the formation, through ultraviolet exposure, of pyrimidine dimers and other lesions which are known to be repaired by transcription-coupled NER<sup>14</sup>.

Beyond these known examples of DNA damage processed by transcription-coupled NER, other signatures show strong transcriptional strand bias (5, 8, 10, 12, 16). Notably, signature 16, which is characterized by T>C mutations at ApTpA, ApTpG and ApTpT trinucleotides and is observed in hepatocellular carcinomas, shows the strongest transcriptional strand bias of any signature, with T>C mutations occurring almost exclusively on the transcribed strand

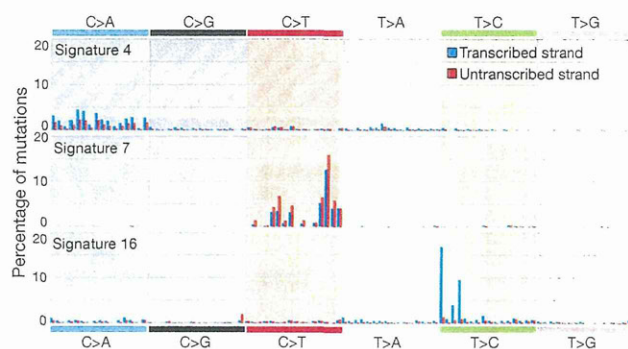


**Figure 5 | Selected mutational signatures with strong transcriptional strand bias.** Mutations are shown according to the 192 mutation classification incorporating the substitution type, the sequence context immediately 5' and 3' to the mutated base and whether the mutated pyrimidine is on the transcribed or untranscribed strand. The mutation types are displayed on the horizontal axis, whereas the vertical axis depicts the percentage of mutations attributed to a specific mutation type. A higher resolution version of all mutational signatures with strong transcriptional strand bias is found respectively in Supplementary Figs 89–95.

(Fig. 5). Similarly, signature 12, which features T>C mutations at NpTpN trinucleotides, also found in hepatocellular carcinomas, shows strong transcriptional strand bias with more T>C mutations on the transcribed than untranscribed strands (Supplementary Fig. 94). On the assumption that the transcriptional strand biases in signatures 12 and 16 are introduced by transcription-coupled NER, these currently unexplained signatures may be the result of bulky DNA helix-distorting adducts on adenine. However, there is no previous basis for invoking transcription-coupled NER in the genesis of these signatures and other causes of transcriptional strand bias may exist.

### Mutational signatures with insertions and deletions

We re-extracted the mutational signatures including, in addition to the 96 substitution types, two further classes of mutation: indels at short nucleotide repeats and indels with overlapping microhomology at breakpoint junctions. Three of the 21 base substitution signatures associated with large numbers of indels. Signature 6, which is characterized predominantly by C>T at NpCpG mutations, but is distinct from signature 1A/B, contributes very large numbers of substitutions and small indels (mostly of 1 bp) at nucleotide repeats to subsets of colorectal, uterine, liver, kidney, prostate, oesophageal and pancreatic cancers. This pattern of indels, often termed ‘microsatellite instability’, is characteristic of cancers with defective DNA mismatch repair<sup>15</sup>. Consistent with this explanation, the presence of signature 6 was strongly associated with the inactivation of DNA mismatch repair genes in colorectal cancer ( $P = 3.3 \times 10^{-5}$ ).

Signature 15 also contributes very large numbers of substitutions and small indels at nucleotide repeats but, compared to signature 6, exhibits greater prominence of C>T at GpCpN trinucleotides. Signature 15 was found in several samples of lung and stomach cancer and its origin is currently unknown.

By contrast, substantial numbers of larger deletions (up to 50 bp) with overlapping microhomology at breakpoint junctions were found in breast, ovarian and pancreatic cancer cases with major contributions from signature 3. A subset of cancer cases of these three classes is known to be due to inactivating mutations in *BRCA1* and *BRCA2*, and the presence of signature 3 was strongly associated with *BRCA1* and *BRCA2* mutations within the individual cancer types ( $P = 1.6 \times 10^{-8}$  for breast cancer and  $P = 0.02$  for pancreatic cancer)<sup>6</sup>. Indeed, almost all cases with *BRCA1* and *BRCA2* mutations showed a large contribution from signature 3. However, some cases with a substantial contribution from signature 3 did not have *BRCA1* and *BRCA2* mutations,



indicating that other mechanisms of *BRCA1* and *BRCA2* inactivation or abnormalities of other genes may also generate it.

*BRCA1* and *BRCA2* are implicated in homologous-recombination-based DNA double-strand break repair<sup>16</sup>. Abrogation of their functions results in non-homologous end-joining mechanisms, which can use microhomology at rearrangement junctions to rejoin double-strand breaks, taking over DNA double-strand break repair. The results show that, in addition to the genomic structural instability conferred by defective double-strand break repair, a base substitution mutational signature is associated with *BRCA1* and *BRCA2* deficiency.

### Associating cancer aetiology and mutational signatures

Each mutational signature is the imprint left on the cancer genome by a mutational process that may include one or more DNA damage and/or DNA maintenance mechanisms, with the latter either functioning normally or abnormally. Here we consider likely mechanisms or underlying causes by comparing signatures with mutation patterns of known causation in the scientific literature or by associating them with epidemiological and biological features of particular cancer types.

Signature 1A/B is probably due to the endogenous mutational process present in most normal and neoplastic cells that is initiated by deamination of 5-methyl-cytosine<sup>9</sup>. Other signatures are probably attributable to exogenous mutagenic exposures. Signature 7 is observed in malignant melanoma and squamous carcinoma of the head and neck and has the known features of ultraviolet-light-induced mutations. Signature 4 is found in cancers associated with tobacco smoking (Fig. 3) and has the mutational features associated with tobacco carcinogens<sup>13</sup>. The causal relationship between tobacco smoking and signature 4 is supported by a strong positive association between smoking history and the contributions of signature 4 to individual cancers ( $P = 1.1 \times 10^{-7}$ , Supplementary Figs 44–46, 74–76 and 96).

Cigarette smoke contains over 60 carcinogens<sup>13</sup> and it is possible that this complex mixture may initiate other mutational processes. Signatures 1A/B, 2 and 5 were also found in lung adenocarcinoma. Signature 5, but not signatures 1A/B and 2, also showed a positive correlation between smoking history and mutation contribution ( $P = 8.0 \times 10^{-3}$ , Supplementary Fig. 96). Thus, in lung cancer, signature 5, which is characterized predominantly by C>T and T>C mutations, may also be due to tobacco carcinogens. However, it is also present in nine other cancer types, most of which are not strongly associated with tobacco consumption, and therefore its aetiology overall is unclear (Fig. 3).

Some anticancer drugs are mutagens<sup>17</sup>. Signature 11 is found in malignant melanomas and glioblastoma multiforme pretreated with the alkylating agent temozolomide ( $P = 4.0 \times 10^{-3}$ ) and has mutational features very similar to those previously reported in experimental studies of alkylating agents<sup>18</sup>.

Abnormalities in DNA maintenance may also be responsible for mutational signatures, and the roles of defective DNA mismatch repair (signature 6) and defective homologous-recombination-based DNA double-strand break repair (signature 3) have been discussed above. Other signatures may result from abnormal activity of enzymes that modify DNA or of error-prone polymerases. Signatures 2 and 13 have been attributed to the AID/APOBEC family of cytidine deaminases<sup>6</sup>. On the basis of similarities in the sequence context of cytosine mutations caused by APOBEC enzymes in experimental systems, a role for APOBEC1, APOBEC3A and/or APOBEC3B in human cancer seems more likely than for other members of the family<sup>19–21</sup>. However, the reason for the extreme activation of this mutational process in some cancers is unknown. Because APOBEC activation constitutes part of the innate immune response to viruses and retrotransposons<sup>22</sup> it may be that these mutational signatures represent collateral damage on the human genome from a response originally directed at retrotransposing DNA elements or exogenous viruses. Confirmation of this hypothesis would establish an important new mechanism for initiation of human carcinogenesis.

Signature 9, observed in chronic lymphocytic leukaemia and malignant B-cell lymphomas, is characterized by T>G transversions at ApTpN and TpTpN trinucleotides, and is restricted to cancers that have undergone somatic immunoglobulin gene hypermutation (IGHV-mutated) associated with AID ( $P = 2.5 \times 10^{-4}$  in chronic lymphoid leukaemia (CLL)). Signature 9 does not, however, have the known mutational features of AID<sup>20</sup>, and has been proposed to be due to polymerase  $\eta$ , an error-prone polymerase involved in processing AID-induced cytidine deamination<sup>11,23</sup>. Similarly, signature 10, which generates huge numbers of mutations in subsets of colorectal and uterine cancer, has been previously associated with altered activity of the error-prone polymerase Pol  $\epsilon$  consequent on mutations in the gene<sup>24,25</sup>.

Many mutational signatures do not, however, have an established or proposed underlying mutational process or aetiology. Some, for example signatures 8, 12 and 16, show strong transcriptional strand bias (Fig. 5) and possibly reflect the involvement of transcription-coupled nucleotide excision repair acting on bulky DNA adducts due to exogenous carcinogens. Others, for example signatures 14, 15 and 21, show overwhelming activity in a small number of cancer cases (Supplementary Figs 38, 45 and 56, respectively) and are perhaps more likely to be due to currently uncharacterized defects in DNA maintenance.

### Localized hypermutation

Foci of localized substitution hypermutation, termed kataegis after the Greek for thunderstorm, were recently described in breast cancer<sup>6</sup>. Kataegis is characterized by clusters of C>T and/or C>G mutations which are substantially enriched at TpCpN trinucleotides and on the same DNA strand. Foci of kataegis include from a few to several thousand mutations and are often found in the vicinity of genomic rearrangements. The genomic regions affected are different in different cancers. On the basis of the substitution types and sequence context of kataegis substitutions, an underlying role for APOBEC family enzymes was proposed for kataegis as well as for signatures 2 and 13 (ref. 6).

The 507 whole-cancer genome mutation catalogues were searched for clusters of mutations. Cancers of breast (67 of 119), pancreas (11 of 15), lung (20 of 24), liver (15 of 88), medulloblastomas (2 of 100), CLL (15 of 28), B-cell lymphomas (21 of 24) and acute lymphoblastic leukaemia (1 of 1) showed occasional (<10), small (<20 mutations) foci of kataegis, whereas acute myeloid leukaemia (0 of 7) and pilocytic astrocytoma (0 of 101) did not. Subsets of breast (7), lung (6) and haematological cancers (3) showed numerous (>10) kataegic foci and two breast and one pancreatic cancer showed major foci of kataegis (>50 mutations) (Fig. 6 and Supplementary Figs 97 and 98).

Kataegic foci are often associated with genomic rearrangements (Supplementary Fig. 98). In yeast, introduction of a DNA double-strand break greatly increases the likelihood of kataegis in its vicinity, indicating a role for such breaks in initiating the process<sup>20</sup>. However, even in cancer cases with kataegis, most rearrangements do not exhibit nearby kataegis, indicating that a double-strand break is not sufficient.

In neoplasms of B-lymphocyte origin, including CLL and many lymphomas, mutation clusters recurrently occurred at immunoglobulin loci. In these cancers the mutation characteristics were different (Supplementary Fig. 98), bearing the hallmarks of somatic hypermutation associated with AID, which is operative during the generation of immunological diversity<sup>20</sup>.

### Discussion

The diversity and complexity of somatic mutational processes underlying carcinogenesis in human beings is now being revealed through mutational patterns buried within cancer genomes. It is likely that more mutational signatures will be extracted, together with more precise definition of their features, as the number of whole-genome sequenced cancers increases and analytical methods are further refined.

The mechanistic basis of some signatures is, at least partially, understood but for many it remains speculative or unknown. Elucidating the



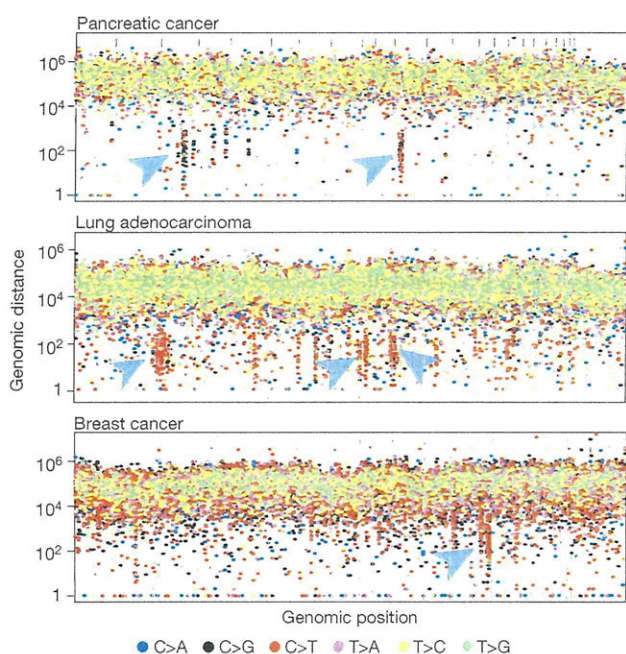


**Figure 6 | Kataegis in three cancers.** Each of these 'rainfall' plots represents an individual cancer sample in which each dot represents a single somatic mutation ordered on the horizontal axis according to its position in the human genome. The vertical axis denotes the genomic distance of each mutation from the previous mutation. Arrowheads indicate clusters of mutations in kataegis.

underlying mutational processes will depend upon two major streams of investigation. First, compilation of mutational signatures from model systems exposed to known mutagens or perturbations of the DNA maintenance machinery and comparison with those found in human cancers. Second, correlation of the contributions of mutational signatures with other biological characteristics of each cancer through diverse approaches ranging from molecular profiling to epidemiology. Collectively, these studies will advance our understanding of cancer aetiology with potential implications for prevention and treatment.

## METHODS SUMMARY

Mutational catalogues were stringently filtered and our previously developed computational framework<sup>5,6</sup> was used to extract mutational signatures from them. The computational framework for deciphering mutational signatures and all mutational catalogues are freely available for download from <http://www.mathworks.com/matlabcentral/fileexchange/38724>, whereas the complete set of somatic mutations is available from <ftp://ftp.sanger.ac.uk/pub/cancer/AlexandrovEtAl>. All presented mutational signatures were validated. Kataegis was detected using an algorithm based on piecewise constant fitting.

**Full Methods** and any associated references are available in the online version of the paper.

Received 24 March; accepted 19 July 2013.

Published online 14 August 2013.

- Stratton, M. R., Campbell, P. J. & Futreal, P. A. The cancer genome. *Nature* **458**, 719–724 (2009).
- Pfeifer, G. P. Environmental exposures and mutational patterns of cancer genomes. *Genome Med.* **2**, 54 (2010).
- Peña-Díaz, J. et al. Noncanonical mismatch repair as a source of genomic instability in human cells. *Mol. Cell* **47**, 669–680 (2012).
- Olivier, M., Hollstein, M. & Hainaut, P. TP53 mutations in human cancers: origins, consequences, and clinical use. *Cold Spring Harb. Perspect. Biol.* **2**, a001008 (2010).
- Alexandrov, L. B., Nik-Zainal, S., Wedge, D. C., Campbell, P. J. & Stratton, M. R. Deciphering signatures of mutational processes operative in human cancer. *Cell Rep.* **3**, 246–259 (2013).
- Nik-Zainal, S. et al. Mutational processes molding the genomes of 21 breast cancers. *Cell* **149**, 979–993 (2012).

- Nik-Zainal, S. et al. The life history of 21 breast cancers. *Cell* **149**, 994–1007 (2012).
- Hudson, T. J. et al. International network of cancer genome projects. *Nature* **464**, 993–998 (2010).
- Pfeifer, G. P. Mutagenesis at methylated CpG sequences. *Curr. Top. Microbiol. Immunol.* **301**, 259–281 (2006).
- Welch, J. S. et al. The origin and evolution of mutations in acute myeloid leukemia. *Cell* **150**, 264–278 (2012).
- Di Noia, J. M. & Neuberger, M. S. Molecular mechanisms of antibody somatic hypermutation. *Annu. Rev. Biochem.* **76**, 1–22 (2007).
- Hanawalt, P. C. & Spivak, G. Transcription-coupled DNA repair: two decades of progress and surprises. *Nature Rev. Mol. Cell Biol.* **9**, 958–970 (2008).
- Pfeifer, G. P. et al. Tobacco smoke carcinogens, DNA damage and p53 mutations in smoking-associated cancers. *Oncogene* **21**, 7435–7451 (2002).
- Pfeifer, G. P., You, Y. H. & Besaratinia, A. Mutations induced by ultraviolet light. *Mutat. Res.* **571**, 19–31 (2005).
- Boland, C. R. & Goel, A. Microsatellite instability in colorectal cancer. *Gastroenterology* **138**, 2073–2087 (2010).
- Thompson, L. H. Recognition, signaling, and repair of DNA double-strand breaks produced by ionizing radiation in mammalian cells: the molecular choreography. *Mutat. Res.* **751**, 153–246 (2012).
- Hunter, C. et al. A hypermutation phenotype and somatic MSH6 mutations in recurrent human malignant gliomas after alkylator chemotherapy. *Cancer Res.* **66**, 3987–3991 (2006).
- Tomita-Mitchell, A. et al. Mismatch repair deficient human cells: spontaneous and MNNG-induced mutational spectra in the HPRT gene. *Mutat. Res.* **450**, 125–138 (2000).
- Taylor, B. J. M. et al. DNA deaminases induce break-associated mutation showers with implication of APOBEC3B and 3A in breast cancer kataegis. *eLife* e00534 (2013).
- Burns, M. B. et al. APOBEC3B is an enzymatic source of mutation in breast cancer. *Nature* **494**, 366–370 (2013).
- Harris, R. S., Petersen-Mahrt, S. K. & Neuberger, M. S. RNA editing enzyme APOBEC1 and some of its homologs can act as DNA mutators. *Mol. Cell* **10**, 1247–1253 (2002).
- Koito, A. & Ikeda, T. Intrinsic immunity against retrotransposons by APOBEC cytidine deaminases. *Front. Microbiol.* **4**, 28 (2013).
- Puente, X. S. et al. Whole-genome sequencing identifies recurrent mutations in chronic lymphocytic leukaemia. *Nature* **475**, 101–105 (2011).
- The Cancer Genome Atlas Network. Comprehensive molecular characterization of human colon and rectal cancer. *Nature* **487**, 330–337 (2012).
- Cancer Genome Atlas Research. Integrated genomic characterization of endometrial carcinoma. *Nature* **497**, 67–73 (2013).
- Lawrence, M. S. et al. Mutational heterogeneity in cancer and the search for new cancer-associated genes. *Nature* **499**, 214–218 (2013).

**Supplementary Information** is available in the online version of the paper.

**Acknowledgements** We would like to thank the Wellcome Trust for support (grant reference 098051) together with many other funding bodies and individuals (Supplementary Note 1).

**Author Contributions** L.B.A., S.N.-Z. and M.R.S. conceptualized the study and analysed the mutational signatures and kataegis data. L.B.A. performed data curation, data filtering and mutational signature extraction. S.N.-Z. and D.C.W. performed kataegis identification. S.N.-Z. performed visual validation. A.P.B., K.R., J.W.T. and D.J. provided bioinformatics support for mutational signature and kataegis analysis. S.A.J.R.A., S.B.E., A.V.B., G.R.B., N.B., A.B., A.-L.B.-D., S.Bo., B.B., C.C., H.R.D., C.D., R.E., J.E.E., J.A.F., M.G., F.H., B.H., T.I., S.I., M.I., N.J., D.T.W.J., S.K., M.K., S.R.L., C.L.-O., S.M., N.C.M., H.N., P.A.N., M.P., E.P., A.P., J.V.P., X.S.P., M.R., A.L.R., J.R., P.R., M.S., T.N.S., P.N.S., Y.T., A.N.J.T., R.V.-M., M.M.V.B., L.V.V., A.V.-S., N.W., L.R.Y., J.Z.-R., P.A.F., U.M., P.L., M.M., S.M.G., R.S., E.C., T.S., S.M.P. and P.J.C. contributed samples, clinical data and scientific advice. M.R.S. and L.B.A. wrote the manuscript. M.R.S. directed the overall research.

**Author Information** The computational framework for deciphering mutational signatures and all mutational catalogues are freely available for download from <http://www.mathworks.com/matlabcentral/fileexchange/38724>, whereas the complete set of somatic mutations is available from <ftp://ftp.sanger.ac.uk/pub/cancer/AlexandrovEtAl>. Reprints and permissions information is available at [www.nature.com/reprints](http://www.nature.com/reprints). The authors declare no competing financial interests. Readers are welcome to comment on the online version of the paper. Correspondence and requests for materials should be addressed to M.R.S. (mrs@sanger.ac.uk).

Ludmil B. Alexandrov<sup>1</sup>, Serena Nik-Zainal<sup>1,2</sup>, David C. Wedge<sup>1</sup>, Samuel A. J. R. Aparicio<sup>3,4,5</sup>, Sam Behjati<sup>1,6</sup>, Andrew V. Biankin<sup>7,8,9,10,11</sup>, Graham R. Bignelli<sup>1</sup>, Niccolò Bolli<sup>1,12,13</sup>, Ake Borg<sup>14</sup>, Anne-Lise Børresen-Dale<sup>15,16</sup>, Sandrine Boyault<sup>17</sup>, Birgit Burkhardt<sup>1,8,19</sup>, Adam P. Butler<sup>1</sup>, Carlos Caldas<sup>20</sup>, Helen R. Davies<sup>1</sup>, Christine Desmedt<sup>21</sup>, Roland Eils<sup>22</sup>, Jörunn Erla Eyfjörð<sup>23</sup>, John A. Foekens<sup>24</sup>, Mel Greaves<sup>25</sup>, Fumie Hosoda<sup>26</sup>, Barbara Hutter<sup>22</sup>, Tomislav Ilčić<sup>1</sup>, Sandrine Imbeaud<sup>27,28</sup>, Marcin Imielinski<sup>29</sup>, Natalie Jäger<sup>22</sup>, David T. W. Jones<sup>30</sup>, David Jones<sup>1</sup>, Stian Knappskog<sup>31,32</sup>, Marcel Kool<sup>30</sup>, Sunil R. Lakhani<sup>33</sup>, Carlos López-Otín<sup>34</sup>, Sancha Martin<sup>1</sup>, Nikhil C. Munshi<sup>35,36</sup>, Hiromi Nakamura<sup>26</sup>, Paul A. Northcott<sup>30</sup>, Marina Pajic<sup>7</sup>, Elli Papaemmanuil<sup>1</sup>, Angelo Paradiso<sup>37</sup>, John V. Pearson<sup>38</sup>, Xose S. Puente<sup>34</sup>, Keiran Raine<sup>1</sup>, Manasa Ramakrishna<sup>1</sup>, Andrea L. Richardson<sup>39,40,41</sup>, Julia Richter<sup>42</sup>, Philip Rosenstiel<sup>43</sup>, Matthias Schlesner<sup>22</sup>, Ton N. Schumacher<sup>44</sup>, Paul N. Span<sup>45</sup>, Jon W.



Teague<sup>1</sup>, Yasushi Totoki<sup>26</sup>, Andrew N. J. Tutt<sup>46</sup>, Rafael Valdés-Mas<sup>34</sup>, Marit M. van Buuren<sup>44</sup>, Laura van 't Veer<sup>47</sup>, Anne Vincent-Salomon<sup>48</sup>, Nicola Waddell<sup>38</sup>, Lucy R. Yates<sup>1</sup>, Australian Pancreatic Cancer Genome Initiative\*, ICGC Breast Cancer Consortium\*, ICGC MMLL-Seq Consortium\*, ICGC PedBrain\*, Jessica Zucman-Rossi<sup>27,28</sup>, P. Andrew Futreal<sup>4</sup>, Ultan McDermott<sup>1</sup>, Peter Lichter<sup>49</sup>, Matthew Meyerson<sup>29,39,40</sup>, Sean M. Grimmond<sup>38</sup>, Reiner Siebert<sup>42</sup>, Elías Campo<sup>50</sup>, Tatsuhiro Shibata<sup>26</sup>, Stefan M. Pfister<sup>30,51</sup>, Peter J. Campbell<sup>1,12,13</sup> & Michael R. Stratton<sup>1</sup>

<sup>1</sup>Cancer Genome Project, Wellcome Trust Sanger Institute, Wellcome Trust Genome Campus, Hinxton, Cambridgeshire CB10 1SA, UK. <sup>2</sup>Department of Medical Genetics, Box 134, Addenbrooke's Hospital NHS Trust, Hills Road, Cambridge CB2 0QQ, UK. <sup>3</sup>Molecular Oncology, Michael Smith Genome Sciences Centre, BC Cancer Agency, 675 West 10th Avenue, Vancouver V5Z 1L3, Canada. <sup>4</sup>Centre for Translational and Applied Genomics, Michael Smith Genome Sciences Centre, BC Cancer Agency, 675 West 10th Avenue, Vancouver V5Z 1L3, Canada. <sup>5</sup>Department of Pathology, University of British Columbia, G227-2211 Wesbrook Mall, British Columbia, Vancouver V6T 2B5, Canada. <sup>6</sup>Department of Paediatrics, University of Cambridge, Hills Road, Cambridge CB2 2XY, UK. <sup>7</sup>Wolfson Wohl Cancer Research Centre, Institute of Cancer Sciences, University of Glasgow, Garscube Estate, Switchback Road, Bearsden, Glasgow G61 1BD, UK. <sup>8</sup>West of Scotland Pancreatic Unit, Glasgow Royal Infirmary, Glasgow G4 0SF, UK. <sup>9</sup>The Kinghorn Cancer Centre, 370 Victoria Street, Darlinghurst, and the Cancer Research Program, Garvan Institute of Medical Research, 384 Victoria Street, Darlinghurst, Sydney, New South Wales 2010, Australia. <sup>10</sup>Department of Surgery, Bankstown Hospital, Eldridge Road, Bankstown, Sydney, New South Wales 2200, Australia. <sup>11</sup>South Western Sydney Clinical School, Faculty of Medicine, University of New South Wales, Liverpool, New South Wales 2170, Australia. <sup>12</sup>Department of Haematology, Addenbrooke's Hospital, Cambridge CB2 0QQ, UK. <sup>13</sup>Department of Haematology, University of Cambridge, Cambridge CB2 2XY, UK. <sup>14</sup>Department of Oncology, Lund University, SE-221 85 Lund, Sweden. <sup>15</sup>Department of Genetics, Institute for Cancer Research, Oslo University Hospital, The Norwegian Radium Hospital, Montebello, 0310 Oslo, Norway. <sup>16</sup>The K.G. Jebsen Center for Breast Cancer Research, Institute for Clinical Medicine, Faculty of Medicine, University of Oslo, N-0310 Oslo, Norway. <sup>17</sup>Plateforme de Bioinformatique Synergie Lyon Cancer, Centre Léon Bérard, 28 rue Laennec, 69373 Lyon Cedex 08, France. <sup>18</sup>NHL-BFM Study Center and Department of Pediatric Hematology and Oncology, University Children's Hospital, 48149 Münster, Germany. <sup>19</sup>NHL-BFM Study Center and Department of Pediatric Hematology and Oncology, University Children's Hospital, 35392 Giessen, Germany. <sup>20</sup>Cancer Research UK Cambridge Institute, University of Cambridge, Li Ka Shing Centre, Cambridge CB2 0RE, UK. <sup>21</sup>Breast Cancer Translational Res Lab -BCTL, Université Libre de Bruxelles—Institut Jules Bordet, Boulevard de Waterloo, 125, B-1000 Brussels, Belgium. <sup>22</sup>Department of Theoretical Bioinformatics (B080), German Cancer Research Center (DKFZ), Im Neuenheimer Feld 280, 69120 Heidelberg, Germany. <sup>23</sup>Cancer

Research Laboratory, Faculty of Medicine, Biomedical Centre, University of Iceland, 101 Reykjavik, Iceland. <sup>24</sup>Department of Medical Oncology, Erasmus MC Cancer Institute, 3015 CE Rotterdam, The Netherlands. <sup>25</sup>Department of Haemato-oncology, Institute of Cancer Research, London SM2 5NG, UK. <sup>26</sup>Division of Cancer Genomics, National Cancer Center Research Institute, Chuo-ku, Tokyo 104-0045, Japan. <sup>27</sup>INSERM, UMR-674, Génomique Fonctionnelle des Tumeurs Solides, Institut Universitaire d'Hématologie (IUH), 75475 Paris, France. <sup>28</sup>Université Paris Descartes, Labex Immuno-oncology, Sorbonne Paris Cité, Faculté de Médecine, 75006 Paris, France. <sup>29</sup>The Broad Institute of MIT and Harvard, Cambridge, Massachusetts 02141, USA. <sup>30</sup>Division of Pediatric Neurooncology, German Cancer Research Center (DKFZ), 69120 Heidelberg, Germany. <sup>31</sup>Section of Oncology, Department of Clinical Science, University of Bergen, 5020 Bergen, Norway. <sup>32</sup>Department of Oncology, Haukeland University Hospital, 5021 Bergen, Norway. <sup>33</sup>The University of Queensland Centre for Clinical Research, School of Medicine and Pathology Queensland, The Royal Brisbane & Women's Hospital, Herston 4029, Brisbane, Queensland, Australia. <sup>34</sup>Departamento Bioquímica y Biología Molecular, IUOPA-Universidad de Oviedo, 33006 Oviedo, Spain. <sup>35</sup>Jerome Lipper Multiple Myeloma Disease Center, Dana-Farber Cancer Institute, Harvard Medical School, Boston, Massachusetts 02215, USA. <sup>36</sup>Boston Veterans Administration Healthcare System, West Roxbury, Massachusetts 02132, USA. <sup>37</sup>Clinical Experimental Oncology Laboratory, National Cancer Institute, Via Amendola, 209, 70126 Bari, Italy. <sup>38</sup>Queensland Centre for Medical Genomics, Institute for Molecular Bioscience, The University of Queensland, St Lucia, Brisbane, Queensland 4072, Australia. <sup>39</sup>Dana-Farber Cancer Institute, 450 Brookline Avenue, Boston, Massachusetts 02215, USA. <sup>40</sup>Harvard Medical School, Boston, Massachusetts 02115, USA. <sup>41</sup>Department of Pathology, Brigham and Women's Hospital, 75 Francis Street, Boston, Massachusetts 02115, USA. <sup>42</sup>Institute of Human Genetics, Christian-Albrechts-University, 24118 Kiel, Germany. <sup>43</sup>Institute of Clinical Molecular Biology, Christian-Albrechts-University, 24118 Kiel, Germany. <sup>44</sup>Division of Immunology, The Netherlands Cancer Institute, Plesmanlaan 121, 1066 CX Amsterdam, The Netherlands. <sup>45</sup>Department of Radiation Oncology and department of Laboratory Medicine, Radboud University Nijmegen Medical Centre, PO Box 9101, 6500HB Nijmegen, The Netherlands. <sup>46</sup>Breakthrough Breast Cancer Research Unit, King's College London School of Medicine, London SW3 6JB, UK. <sup>47</sup>The Netherlands Cancer Institute, 121 Plesmanlaan, 1066 CX Amsterdam, The Netherlands. <sup>48</sup>Institut Curie, Département de Pathologie, INSERM U830, 26 rue d'Ulm, 75248 Paris Cedex 05, France. <sup>49</sup>Division of Molecular Genetics, German Cancer Research Center (DKFZ), 69120 Heidelberg, Germany. <sup>50</sup>Unidad de Hematopatología, Servicio de Anatomía Patológica, Hospital Clínic, Universitat de Barcelona, IDIBAPS, 08036 Barcelona, Spain. <sup>51</sup>Department of Pediatric Hematology and Oncology, 69120 Heidelberg, Germany.

\*A list of authors and affiliations appears in the Supplementary Information.



## METHODS

**Validating mutational signatures.** Validating a mutational signature requires ensuring that a large set of somatic mutations attributed to this signature is genuine in at least one sample. Validation is complicated as multiple mutational processes are usually operative in most cancer samples, and thus every individual somatic mutation can be probabilistically assigned to several mutational signatures. To overcome this limitation, we examined our data set for samples that are predominantly generated by one mutational signature (that is, more than 50% of the somatic mutations in the sample belong to an individual mutational signature) and/or for samples in which all operative mutational processes have mutually exclusive patterns of mutations (for example, a sample with mutations only from signature 1B, which is predominantly C>T substitutions, and signature 18, which is predominantly C>A substitutions). We identified the optimal available sample for every mutational signature and attempted to validate the subset of somatic mutations attributed to this signature using one of three methods (Supplementary Fig. 99): (1) validation through re-sequencing with an orthogonal sequencing technology; (2) validation through re-sequencing with the same sequencing technology (including RNA-seq, bisulphite sequencing, etc.); (3) validation through visual examination of somatic mutations by an experienced curator using a genomic browser and BAM files for both the tumour and its matched normal.

For some of the previously published samples, we used the already reported validation data. When possible, somatic mutations were validated by either re-sequencing with orthogonal technology or re-sequencing using the same sequencing technology. We resorted to visual validation only when there was no other possibility for validating a mutational signature. 22 out of the 27 originally identified mutational signatures were validated (Supplementary Table 1 and Supplementary Fig. 99). Three mutational signatures failed validation: signatures R1 to R3 (Supplementary Figs 24 to 26). We were unable to validate two mutational signatures: signatures U1 and U2 (Supplementary Figs 27 and 28), due to lack of available biological samples and access to BAM files for the samples with sufficient number of somatic mutations generated by these two mutational signatures.

**Samples and curation of freely available cancer data.** Informed consent was obtained from all subjects. Collection and use of patient samples were approved by the appropriate Internal Review Board of each institution. In addition to newly generated data, we curated freely available somatic mutations from three other sources: (1) the data portal of The Cancer Genome Atlas (TCGA); (2) the data portal of the International Cancer Genome Consortium (ICGC); (3) previously published data in peer-review journals, see additional references<sup>6,23,27–29</sup>.

**Filtering, estimating mutation prevalence and generating mutational catalogues.** In all examined samples, normal DNA from the same individuals had been sequenced to establish the somatic origin of variants. Extensive filtering was performed to remove any residual germline mutations and technology-specific sequencing artefacts before analysing the data. Germline mutations were filtered out from the lists of reported mutations using the complete list of germline mutations from dbSNP<sup>60</sup>, 1000 genomes project<sup>61</sup>, NHLBI GO Exome Sequencing Project<sup>62</sup>, and 69 Complete Genomics panel (<http://www.completegenomics.com/public-data/69-Genomes/>). Technology-specific sequencing artefacts were filtered out by using panels of BAM files of (unmatched) normal tissues containing more than 120 normal genomes and 500 normal exomes. Any somatic mutation present in at least three well-mapping reads in at least two normal BAM files was discarded. The remaining somatic mutations were used for generating a mutational catalogue for every sample.

Prevalence of somatic mutations was estimated on the basis of a haploid human genome after all filtering. Prevalence of somatic mutations in exomes was calculated based on the identified mutations in protein-coding genes and assuming that an average exome has 30 Mb in protein-coding genes with sufficient coverage. Prevalence of somatic mutations in whole genomes was calculated based on all identified mutations and assuming that an average whole genome has 2.8 gigabases with sufficient coverage.

The immediate 5' and 3' sequence context was extracted using the ENSEMBL Core programming interfaces for human genome build GRCh37. Curated somatic mutations that originally mapped to an older version of the human genome were re-mapped using UCSC's freely available lift genome annotations tool (any somatic mutations with ambiguous or missing mappings were discarded). Dinucleotide substitutions were identified when two substitutions were present in consecutive bases on the same chromosome (sequence context was ignored). The immediate 5' and 3' sequence content of all indels was examined and the ones present at mono/polynucleotide repeats or microhomologies were included in the analysed mutational catalogues as their respective types. Strand bias catalogues were derived for each sample using only substitutions identified in the transcribed regions of well-annotated protein-coding genes. Genomic regions of bidirectional transcription were excluded from the strand bias analysis.

**Deciphering signatures of mutational processes.** Mutational signatures were deciphered independently for each of the 30 cancer types using our previously

developed computational framework<sup>5</sup>. The algorithm deciphers the minimal set of mutational signatures that optimally explains the proportion of each mutation type found in each catalogue and then estimates the contribution of each signature to each catalogue. Mutational signatures were also extracted separately for genomes and exomes. Mutational signatures extracted from exomes were normalized using the observed trinucleotide frequency in the human exome to the one of the human genome. All mutational signatures were clustered using unsupervised agglomerative hierarchical clustering and a threshold was selected to identify the set of consensus mutational signatures. Mis-clustering was avoided by manual examination (and whenever necessary re-assignment) of all signatures in all clusters. 27 consensus mutational signatures were identified across the 30 cancer types. The computational framework for deciphering mutational signatures as well as the data used in this study are freely available and can be downloaded from <http://www.mathworks.com/matlabcentral/fileexchange/38724>, whereas the complete set of somatic mutations is available from <ftp://ftp.sanger.ac.uk/pub/cancer/AlexandrovEtAl>.

**Factors that influence extraction of mutational signatures.** Recently, using simulated and real data, we described in detail the factors that influence the extraction of mutational signatures<sup>5</sup>. These included the number of available samples, the mutation prevalence in samples, the number of mutations contributed by different mutational signatures, the similarity between the signatures of mutational processes operative in cancer samples, as well as the limitations of our computational approach. Here, we examined data sets with varying sizes from 30 different cancer types and we have taken great care to report only validated mutational signatures. However, our approach identified two similar patterns most likely representing the same biological process; that is, signature 1A and 1B. The reasons for this is, for some cancer types we have sufficient numbers of samples and/or mutations (that is, statistical power) to decipher the cleaner version (that is, signature 1A), whereas for other cancer types we do not have sufficient data and our approach extracts a version of the signature which is more contaminated by other signatures present in that cancer type (that is, signature 1B). Nevertheless, the two signatures are very similar; hence we call them 1A and 1B. Being almost mutually exclusive among cancer types (that is, finding either signature 1A or 1B in each cancer type but not usually both) is supportive of the notion that they represent the same underlying process as is the fact that signatures 1A and 1B both correlate with age and have the same overall pattern of contributions to individual cancer genomes. Indeed, in our view it is likely that if we had sufficient data, signature 1B would disappear and the algorithm would extract only signature 1A.

**Displaying mutational signatures.** Mutational signatures are displayed using a 96 substitution classification defined by the substitution class and the sequence context immediately 3' and 5' to the mutated base. Mutational signatures are displayed in the main text of the report and in Supplementary Information on the basis of the observed trinucleotide frequency of the human genome; that is, representing the relative proportions of mutations generated in each signature based on the actual trinucleotide frequencies of the reference human genome. However, in Supplementary Information we also provide a visualization of mutational signatures based on an equal frequency of each trinucleotide (Supplementary Figs 2–28). The equal trinucleotide frequency representation results, in all mutational signatures, in a greater degree of prominence of C>T substitutions at NpCpG trinucleotides as major features compared to the plots based on the observed trinucleotides. This difference may in some cases reflect the biological reality, that is, a propensity of the particular mutational process to be more active at NpCpG trinucleotides. However, note that it may also in some cases be due to incomplete extraction by the algorithm of the signature in question from signature 1A/B, which is characterized by prominent features at NpCpG trinucleotides. This is likely to happen because (1) signature 1A/B is ubiquitous and (2) because even a small probability of mutations at NpCpG trinucleotides will generate a prominent feature because of the severe depletion of NpCpG trinucleotides in the reference genome. In future, with larger numbers of sequences and large numbers of whole-genome sequences it is anticipated that the latter effect will be reduced.

**Approaches for associating cancer aetiology and exposures of validated mutational signatures.** Generalized linear models (GLMs) were used to fit signature exposures (that is, number of mutations assigned to a signature) and age of cancer diagnoses. For each cancer type, all mutational signatures operative in it were evaluated using GLMs and the *P* values were corrected for multiple hypothesis testing using the Benjamini–Hochberg false discovery rate procedure. The resulting *P* values indicate that age strongly correlates with signature 1A/B across 15 cancer types (Supplementary Table 2). Exposure to signature 4 also correlates with age of diagnosis in kidney papillary and thyroid cancers. However, in both cancer types, we were not able to detect/extract signature 1A/B due to a low number of mutations in their samples and it is likely that signature 1A/B is



currently mixed within signature 4. Further studies involving whole-genome sequences will be needed to validate this hypothesis. Notably, in melanoma, age of diagnosis also correlates with exposure to signature 7, which we have associated with exposure to ultraviolet light.

Associations between all other aetiologies and signature exposures were performed using two-sample Kolmogorov–Smirnov tests between two sets of samples. The first set contains the signature exposures of the samples with the ‘desired feature’ (for example, samples that contain a hypermutation in the immunoglobulin gene) and the second set is the signature exposures of the samples without the ‘desired feature’ (for example, samples that do not contain a hypermutation in the immunoglobulin gene). Samples with unknown feature status (for example, not knowing the status of the immunoglobulin gene) were ignored. Kolmogorov–Smirnov tests were performed for all signatures and all examined ‘features’ in a cancer type. *P* values were corrected for multiple hypothesis testing using the Benjamini–Hochberg false discovery rate procedure and based on the performed tests in a particular cancer class.

**A piecewise-constant-fitting-based algorithm for the detection of kataegis.** Foci of localized hypermutation, termed kataegis, were sought in 507 whole-genome sequenced cancers. High-quality variant calls that had been previously subjected to filtering for mutational signature analysis were investigated using an algorithm developed to identify foci of kataegis.

For each sample, all mutations were ordered by chromosomal position and the intermutation distance, defined as the number of base pairs from each mutation to the next one, was calculated. Intermutation distances were then segmented using the piecewise constant fitting (PCF) method<sup>63</sup> to find regions of constant intermutation distance. Parameters used for PCF were  $\gamma = 25$  and  $k_{\min} = 2$  and were trained on the set of kataegis foci that had been manually identified, curated and validated using orthogonal sequencing platforms<sup>6</sup>. Putative regions of kataegis were identified as those segments containing six or more consecutive mutations with an average intermutation distance of less than or equal to 1,000 bp.

**Variation in number of foci of kataegis and relationship with genome-wide mutation burden.** To examine the likelihood of kataegis occurring for different mutation burdens, the expected number of kataegis events that would be observed by chance was calculated for a range of total number of mutations per cancer, *n*, between 1,000 and 2,000,000. The probability that any one mutation will be followed by five other mutations within a distance of 5,000 bp, thereby triggering the identification of kataegis, is given by  $p = P(\text{Pois}(5,000n/g) \geq 5)$ , where *g* is the length of the genome, in base pairs.

Supplementary Fig. 97 shows the expected number of kataegis events identified in genomes with between 100,000 and 500,000 mutations. For cancers with up to 200,000 mutations, the expected number of kataegis events is extremely small (0.16 for a total mutation load of 200,000), making the detection of kataegis foci highly significant for each sample. Supplementary Table 3 presents all the samples in which kataegis foci were identified, the total mutation burden for each sample, the observed number of kataegis foci, and the expected number of foci.

**Specificity of variants in kataegis foci.** Clusters of variant calls can easily occur in regions of low sequence complexity. These are not true substitution mutations but represent systematic sequencing artefacts or mis-mapping of short reads. The quality of variant calls depends on the quality of mutation-calling by individual institutions. Additional filtering was applied to remove likely false-positive calls and then putative kataegis foci were individually curated.

1,436 kataegis foci were called by PCF, with 873 finalized as putative kataegis foci (Supplementary Table 4) involving 9,219 substitution variants. Where possible, BAM files were retrieved, inspected and substitution variants involved in kataegis foci were manually curated to remove likely false-positive calls. Where BAM files were not available to us, substitution variants were strictly excluded if called in: (1) genomic features that generate mapping errors, for example, regions of excessively high coverage due to collapsed repeat sequences in the reference genome<sup>64</sup>; (2) highly repetitive regions with reads consistently demonstrating low mapping qualities in 20 unrelated normal samples; (3) locations with known germline insertions/deletions within the sequencing reads reporting the mutated base.

Several features were seen in the finalized putative kataegis foci, which reinforced the conviction in the validity of these calls. Although clusters of mutations identified by the PCF method were sought in an approach unbiased by mutation type and based exclusively on intermutation distances, we find that the 873 putative foci demonstrate: first, a preponderance to C>T and C>G mutations (Supplementary Fig. 97b); second, the enrichment for a TpC sequence context as previously described<sup>6</sup> (Supplementary Fig. 97b); third, processivity (where consecutive mutations within a cluster were on the same strand; that is, 6 C>T mutations in a row or 6 G>A mutations in a row; Fig. 6c); and fourth, visual curation of reads carrying these processive variants showed that the variants were usually in *cis* (that is, mutations were on the same read (Supplementary Fig. 97c) or on the read mate of other affected alleles within the insert size) with respect to

each other, indicating that they had arisen on the same allele. Finally, where data were available, we found that clusters of substitution mutations within the same kataegis foci shared approximately the same variant allele fraction, indicating that they had probably arisen during a single cell cycle event.

BAM files from some samples were not accessible and therefore a proportion of substitution variants involved in kataegis foci were not visually curated. The application of the strict criteria described above and the subsequent finding of the consistency of the mutation-type, sequence context, processive nature of the mutations, with the majority in *cis* on individual sequencing reads, indicates that the vast majority of these foci are probably genuine. However, the possibility that some of the foci are not truly kataegis, particularly for the cancers which have not been validated or visually curated, remains.

**Sensitivity of kataegis detection.** It is acknowledged that the likelihood of detection of kataegis foci rests on the sensitivity of mutation detection. It is possible for foci to be missed because the mutations were not detected by mutation callers of the various institutions, before our analysis. This is particularly relevant for subclonal mutations bearing a low variant allele fraction or for mutations that occur on a single copy of a multi-copy locus. This is because the likelihood of mutation detection is reduced when uncorrected for copy number and for aberrant cell fraction of the tumour sample. Furthermore, our stringent post-processing criteria, particularly of samples that have not been visually curated, make it more likely that kataegis is under-represented in this analysis.

**Relationship between kataegis and large-scale genomic changes.** Reinforcing our previous findings<sup>6</sup>, we found that some kataegis foci were very closely associated with rearrangements. For example, a breast cancer sample with 1,534 point mutations had only one focus of kataegis which contained 32 point mutations. The same breast cancer sample also had 25 large-scale genomic structural variations scattered throughout the genome. However, one tandem duplication coincided with this single locus of kataegis in this cancer. Notably, no other mutations or structural variations were seen for 2 Mb flanking this extraordinary event (Supplementary Fig. 97b). Another breast cancer (Fig. 6) that contained 22,454 mutations and had 292 rearrangements altogether, had nine regions of kataegis, five of which coincided with large-scale structural variations, underscoring the co-localization of kataegis foci with structural variations. This also highlights that not all foci of kataegis co-localized with structural variations and not all structural variations were associated with kataegis.

Sites of amplification represent a potential source of false variant calls. If the amplification occurred early in the evolution of a cancer, then there is an increased likelihood of substitutions accumulating randomly within the amplified genomic region. When mapped back to the reference genome, these will appear as clustered variants.

A number of features allow us to distinguish such events from ‘true’ kataegis. These mutations would not be expected to have features associated with kataegis, such as the mutation type, predilection for a TpC sequence context and the processivity. Furthermore, if they have accumulated as random events in a multi-copy locus, then they would be less likely to occur in *cis* (on the same sequencing read) with respect to each other. In contrast, mutations which have occurred at the same time, during one moment of transient hypermutability in a single cell cycle event, would be expected to cluster on one copy of a multi-copy locus, to be in *cis* and to demonstrate approximately the same variant allele fraction. Finally, to achieve the level of hypermutation required to be called as a focus of kataegis (average intermutation distance of less than 1,000 bp for six consecutive mutations equivalent to ~1,000 substitutions per Mb), the degree of copy number amplification would have to be considerable.

To examine this likelihood of false calls in regions of amplification, simulations were performed assuming background mutation rates of 10 per Mb, 40 per Mb and 100 per Mb for different copy number states and for different sizes of focal amplification. The expected number of kataegis foci for these different states are provided in Supplementary Table 5. For most of the samples in which kataegis was detected (all but twenty), a 10 Mb region of amplification would require a copy number state of 36 or above to generate 1 cluster of 6 mutations with an average intermutation distance of less than 1,000 bp. For 19 of the remaining 20 samples, a 10 Mb region of amplification would require a copy number state of 10 or above. For the single cancer with a mutation rate exceeding 40 per Mb, a copy number state of 4 is required to generate a cluster of mutations. As mentioned previously, these clusters would have to be processive, be in *cis* and have roughly the same variant allele fraction to be called as a focus of kataegis.

**Definition of kataegis.** Kataegis has been identified via a PCF-based method as 6 or more consecutive mutations with an average intermutation distance of less than or equal to 1,000 bp. Other salient features include a preponderance for C>T and C>G mutations, a predilection for a TpC mutation context, processivity, evidence of having arisen on the same parental allele (being in *cis*) on sequencing reads and additionally (but not necessarily) co-localization with large-scale genomic structural variation.



27. Holmfeldt, L. *et al.* The genomic landscape of hypodiploid acute lymphoblastic leukemia. *Nature Genet.* **45**, 242–252 (2013).
28. Zhang, J. *et al.* The genetic basis of early T-cell precursor acute lymphoblastic leukaemia. *Nature* **481**, 157–163 (2012).
29. De Keersmaecker, K. *et al.* Exome sequencing identifies mutation in CNOT3 and ribosomal genes RPL5 and RPL10 in T-cell acute lymphoblastic leukemia. *Nature Genet.* **45**, 186–190 (2013).
30. Ding, L. *et al.* Clonal evolution in relapsed acute myeloid leukaemia revealed by whole-genome sequencing. *Nature* **481**, 506–510 (2012).
31. Stephens, P. J. *et al.* The landscape of cancer genes and mutational processes in breast cancer. *Nature* **486**, 400–404 (2012).
32. Quesada, V. *et al.* Exome sequencing identifies recurrent mutations of the splicing factor SF3B1 gene in chronic lymphocytic leukemia. *Nature Genet.* **44**, 47–52 (2012).
33. Seshagiri, S. *et al.* Recurrent R-spondin fusions in colon cancer. *Nature* **488**, 660–664 (2012).
34. Dulak, A. M. *et al.* Exome and whole-genome sequencing of esophageal adenocarcinoma identifies recurrent driver events and mutational complexity. *Nature Genet.* **45**, 478–486 (2013).
35. Agrawal, N. *et al.* Exome sequencing of head and neck squamous cell carcinoma reveals inactivating mutations in NOTCH1. *Science* **333**, 1154–1157 (2011).
36. Stransky, N. *et al.* The mutational landscape of head and neck squamous cell carcinoma. *Science* **333**, 1157–1160 (2011).
37. Guo, G. *et al.* Frequent mutations of genes encoding ubiquitin-mediated proteolysis pathway components in clear cell renal cell carcinoma. *Nature Genet.* **44**, 17–19 (2012).
38. Peña-Llopis, S. *et al.* BAP1 loss defines a new class of renal cell carcinoma. *Nature Genet.* **44**, 751–759 (2012).
39. Ding, L. *et al.* Somatic mutations affect key pathways in lung adenocarcinoma. *Nature* **455**, 1069–1075 (2008).
40. Seo, J. S. *et al.* The transcriptional landscape and mutational profile of lung adenocarcinoma. *Genome Res.* **22**, 2109–2119 (2012).
41. Imielinski, M. *et al.* Mapping the hallmarks of lung adenocarcinoma with massively parallel sequencing. *Cell* **150**, 1107–1120 (2012).
42. Love, C. *et al.* The genetic landscape of mutations in Burkitt lymphoma. *Nature Genet.* **44**, 1321–1325 (2012).
43. Zhang, J. *et al.* Whole-genome sequencing identifies genetic alterations in pediatric low-grade gliomas. *Nature Genet.* **45**, 602–612 (2013).
44. Morin, R. D. *et al.* Frequent mutation of histone-modifying genes in non-Hodgkin lymphoma. *Nature* **476**, 298–303 (2011).
45. Jiao, Y. *et al.* DAXX/ATRX, MEN1, and mTOR pathway genes are frequently altered in pancreatic neuroendocrine tumors. *Science* **331**, 1199–1203 (2011).
46. Pugh, T. J. *et al.* The genetic landscape of high-risk neuroblastoma. *Nature Genet.* **45**, 279–284 (2013).
47. Jones, S. *et al.* Frequent mutations of chromatin remodeling gene ARID1A in ovarian clear cell carcinoma. *Science* **330**, 228–231 (2010).
48. Wu, J. *et al.* Whole-exome sequencing of neoplastic cysts of the pancreas reveals recurrent mutations in components of ubiquitin-dependent pathways. *Proc. Natl Acad. Sci. USA* **108**, 21188–21193 (2011).
49. Sausen, M. *et al.* Integrated genomic analyses identify ARID1A and ARID1B alterations in the childhood cancer neuroblastoma. *Nature Genet.* **45**, 12–17 (2013).
50. Berger, M. F. *et al.* The genomic complexity of primary human prostate cancer. *Nature* **470**, 214–220 (2011).
51. Grasso, C. S. *et al.* The mutational landscape of lethal castration-resistant prostate cancer. *Nature* **487**, 239–243 (2012).
52. Barbieri, C. E. *et al.* Exome sequencing identifies recurrent SPOP, FOXA1 and MED12 mutations in prostate cancer. *Nature Genet.* **44**, 685–689 (2012).
53. Rudin, C. M. *et al.* Comprehensive genomic analysis identifies SOX2 as a frequently amplified gene in small-cell lung cancer. *Nature Genet.* **44**, 1111–1116 (2012).
54. Peifer, M. *et al.* Integrative genome analyses identify key somatic driver mutations of small-cell lung cancer. *Nature Genet.* **44**, 1104–1110 (2012).
55. Stark, M. S. *et al.* Frequent somatic mutations in MAP3K5 and MAP3K9 in metastatic melanoma identified by exome sequencing. *Nature Genet.* **44**, 165–169 (2012).
56. Berger, M. F. *et al.* Melanoma genome sequencing reveals frequent PREX2 mutations. *Nature* **485**, 502–506 (2012).
57. Hodis, E. *et al.* A landscape of driver mutations in melanoma. *Cell* **150**, 251–263 (2012).
58. Zang, Z. J. *et al.* Exome sequencing of gastric adenocarcinoma identifies recurrent somatic mutations in cell adhesion and chromatin remodeling genes. *Nature Genet.* **44**, 570–574 (2012).
59. Wang, K. *et al.* Exome sequencing identifies frequent mutation of ARID1A in molecular subtypes of gastric cancer. *Nature Genet.* **43**, 1219–1223 (2011).
60. Sherry, S. T. *et al.* dbSNP: the NCBI database of genetic variation. *Nucleic Acids Res.* **29**, 308–311 (2001).
61. Abecasis, G. R. *et al.* An integrated map of genetic variation from 1,092 human genomes. *Nature* **491**, 56–65 (2012).
62. Fu, W. *et al.* Analysis of 6,515 exomes reveals the recent origin of most human protein-coding variants. *Nature* **493**, 216–220 (2013).
63. Baumbusch, L. O. *et al.* Comparison of the Agilent, ROMA/NimbleGen and Illumina platforms for classification of copy number alterations in human breast tumors. *BMC Genomics* **9**, 379 (2008).
64. Pickrell, J. K., Gaffney, D. J., Gilad, Y. & Pritchard, J. K. False positive peaks in ChIP-seq and other sequencing-based functional assays caused by unannotated high copy number regions. *Bioinformatics* **27**, 2144–2146 (2011).

## Exploration of liver cancer genomes

Tatsuhiko Shibata and Hiroyuki Aburatani

**Abstract** | Liver cancer is the third leading cause of cancer-related death worldwide. Advances in sequencing technologies have enabled the examination of liver cancer genomes at high resolution; somatic mutations, structural alterations, HBV integration, RNA editing and retrotransposon changes have been comprehensively identified. Furthermore, integrated analyses of trans-omics data (genome, transcriptome and methylome data) have identified multiple critical genes and pathways implicated in hepatocarcinogenesis. These analyses have uncovered potential therapeutic targets, including growth factor signalling, WNT signalling, the NFE2L2-mediated oxidative pathway and chromatin modifying factors, and paved the way for new molecular classifications for clinical application. The aetiological factors associated with liver cancer are well understood; however, their effects on the accumulation of somatic changes and the influence of ethnic variation in risk factors still remain unknown. The international collaborations of cancer genome sequencing projects are expected to contribute to an improved understanding of risk evaluation, diagnosis and therapy for this cancer.

Shibata, T. & Aburatani, H. *Nat. Rev. Gastroenterol. Hepatol.* advance online publication 28 January 2014; doi:10.1038/nrgastro.2014.6

### Introduction

Liver cancer is the third leading cause of cancer-related death worldwide.<sup>1</sup> Hepatocellular carcinoma (HCC) is the most common form of liver cancer, followed by intrahepatic cholangiocarcinoma (IHCC).<sup>1</sup> Chronic liver damage, such as that caused by chronic hepatitis, liver cirrhosis and fatty liver disease, is closely associated with the occurrence of liver cancers. Hepatitis virus infection (for example HBV, HCV and others), aflatoxin B exposure, alcohol intake, and other metabolic diseases (such as obesity, diabetes mellitus and haemochromatosis) are well-known risk factors for liver cancer.<sup>2–4</sup> In addition, parasites such as liver fluke are associated with IHCC in Southeast Asian countries.<sup>5,6</sup>

The incidence of liver cancer is high in East Asian and African countries.<sup>1–3,5</sup> HBV infection is more prevalent in Africa and Asian countries (except Japan) than other regions of the world.<sup>3</sup> However, the number of patients infected with HCV has been rapidly increasing in Japan and Western countries, especially in the USA where viral hepatitis infection is partly mediated through drug abuse.<sup>2,3</sup> In this Review, we mainly focus on HCC, as HCC and IHCC showed distinctive genomic alterations and fairly little is known about the IHCC genome alterations at present.

### Somatic alterations in the liver cancer genome

The liver cancer genome contains multiple types of somatic alterations, including mutations (such as single nucleotide substitutions, and small insertions and deletions), changes of gene copy numbers (copy number loss, gain and amplification), and intra-chromosomal

and inter-chromosomal rearrangements (large deletion, inversion, tandem duplication and translocation).

### Genome-wide copy number analysis

Copy number changes in human cancers have been analysed mainly by array-based comparative genome hybridization methods. Bacterial artificial chromosome (BAC) clone DNA or oligonucleotide probe arrays (microarray-based comparative genomic hybridization) have been used in a number of studies to search for copy number changes in liver cancer.<sup>7–20</sup> Table 1 summarizes recurrent copy number alterations in HCC. In addition to well-known oncogenes, such as *MYC* and *CCND1*, and tumour suppressor genes, such as *TP53* and *RB*, liver cancers harbour multiple chromosomal amplifications and deletions.

The identification of target genes solely by copy number data has been challenging. Therefore, strategies based on integrative analysis of genetic alterations, gene expression profiling and oncogenic function of candidate genes might be an effective approach. Zender *et al.*<sup>21</sup> selected potential tumour suppressor genes using data from copy number analyses of human HCC, and functionally identified novel tumour suppressor genes, including *XPO4*, by *in vivo* short hairpin RNA screening in a mosaic mouse model. Sawey *et al.*<sup>22</sup> extracted genes located in chromosomal regions of recurrent focal amplification in human HCC and tested their oncogenic activity using a mouse hepatoblast model. These authors identified 18 tumour-promoting genes, including *FGF19*, which is located next to the *CCND1* gene on 11q13.3. *FGF19* and *CCND1* cooperatively promote tumour formation through the *CTNNB1* pathway.<sup>22</sup>

Katoh *et al.*<sup>13</sup> attempted to define a molecular classification of HCC on the basis of the copy number

Division of Cancer Genomics, National Cancer Center Research Institute, Chuo-ku, Tokyo 104-0045, Japan (T. Shibata). Research Center for Advanced Science and Technology, The University of Tokyo, 4-6-1, Komaba, Meguro-ku, Tokyo 153-8904, Japan (H. Aburatani).

Correspondence to: T. Shibata  
tashibat@ncc.go.jp

### Competing interests

The authors declare no competing interests.